Analyst

Accepted Manuscript

This article can be cited before page numbers have been issued, to do this please use: Q. Li, F. Zeng, N. Lyu and J. Liang, *Analyst*, 2018, DOI: 10.1039/C8AN00437D.

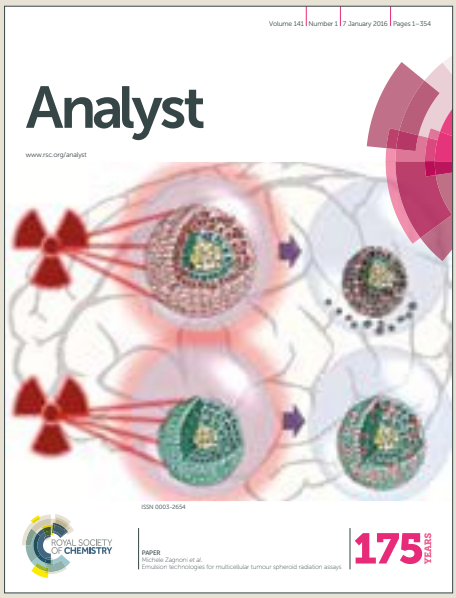

ROYAL SOCIETY OF CHEMISTRY

rsc.li/analyst

View Article Online
DOI: 10.1039/C8AN00437D

Highly sensitive and specific electrochemical biosensor for microRNA 21 coupling catalytic hairpin assembly with rolling circle amplification

Qing Li[1§], Fanpeng Zeng,[1§] Nan Lyu[1*] and Jun Liang[1*]

[1] Xuzhou Central Hospital, Xuzhou, Jiangsu 221004, China

[§]These authors contributed equally to this work and should be considered co-first authors

*Corresponding author: Nan Lyu

E-mail address: lyunan8833@sina.com

**Corresponding author: Jun Liang

E-mail address: mwlj521@163.com

Xuzhou Central Hospital, Xuzhou, Jiangsu 221004, China

View Article Online
DOI: 10.1039/C8AN00437D

ABSTRACT

Background MicroRNA plays a significant role in gene regulation and usually regarded as an important biological marker. Electrochemical biosensor is an excellent tool for microRNA detection.

Methods In this experiment, we take miRNA 21 as target, combining Catalytic hairpin assembly (CHA) and rolling circle amplification (RCA) as dual signal amplification strategy for detection of microRNA on electrochemical biosensor.

Results This strategy has a good linear within 0.5~12500 pmol concentration of microRNA. The limit of detection (LOD) for miRNA is as low as 290 fmol showing excellent performance. Finally, this method has been successfully applied into the detection of miRNA 21 from Hela cell.

Conclusion This method can apply not only in microRNA detection with high sensibility and speed, but also working in the detection of small molecule and protein combing with aptamer.

Key words: catalytic hairpin assembly; rolling circle amplification; electrochemical biosensor; microRNA 21

View Article Online
DOI: 10.1039/C8AN00437D

1. INTRODUCTION

MoicroRNA (miRNAs) is a type of small non-coding RNA molecules with less than 22 nucleotides.[1-4] It is endogenous and conserved, which modulates the gene expression by binding to target mRNAs, leading to translation blockade or target transcripts degradation.[5] Until now, over 2000 kinds of human miRNA have been found to regulate 30% of human gene.[6] In particular, miRNA is the dominant in deadenylation, which reduces the stability of mRNA, thereby effects the translation efficiency and downstream product of proteins. This regulatory mechanism enabled miRNA to be an important potential biomarkers in mediating tumor metastasis, stem-cell differentiation, and viral replication.[7-9] Over the past decades, miRNA has been reported abnormal expression in various cancers, involving gastric cancer, lung cancer, and breast cancer, etc, and other diseases such as cardiovascular disease, degenerative disease, and endocrine disease, etc.[10-12] Thus, it is necessary to develop a sensitive strategy to analyze the miRNA expression for clinical diagnosis.

At present, the detection of miRNA is quite challenging by reason of their small size, assailable degradability, highly homologous sequences, and relatively low expression levels in cells. Traditional techniques, such as northern blotting, real-time PCR, and microarrays, suffer from some disadvantages in practical applications.[13-15] They require extremely precise instrument and have a relatively low sensitivity with time-consuming operation. To avoid these limits, the electrochemical biosensor technique has become very powerful and attracted much attention.[16,17] It has high sensitivity and selectivity, which is suitable for the detection of trace bio-molecules. In addition, several other groups have also developed variety of amplification strategies to continually improve the sensitivity of biosensors, such as rolling circle amplification (RCA), catalytic hairpin assembly (CHA), hybridization chain reaction

View Article Online
DOI: 10.1039/C8AN00437D

(HCR), and loop-mediated isothermal amplification (LAMP), etc.[18-21] Among these strategies, CHA is the most popular amplification techniques with simple isothermal DNA amplification process.[22] Moreover, it is an enzyme-free amplification method which overcomes the complex operation, specific reaction conditions, and the reaction time dependent enzyme activity.[23-25] However, the nonspecific CHA products usually caused great background signal, which severely limited the amplification efficiency. Therefore, other techniques can be used as the combination to supply the amplification. RCA is the simple and rapid DNA reproduction method under the normal laboratory conditions. In RCA amplification, thousands of detection sites can be generated from each template to achieve a mass of ssDNA molecules. Thus, it can be combined to CHA to increase the expansion efficiency by dual amplification.[26,27]

In this work, we have developed a novel dual amplification strategy for the analysis of microRNA 21.[28-32] This amplification is based on the combination of CHA and RCA techniques to achieve high sensitivity, selectivity, and simple operation. The hairpin H1 is partially hybridizes with miR-21 in CHA. So it can be opened to start the CHA reaction when miR-21 exists, and the RCA can be continually used to amplify the response signal. This strategy has a good linear within 0.5~12500 pmol concentration of miR-21 with a low detection limit of 290 fmol. Our method is not only can be applied to microRNA detection with high sensibility and speed, but also in the detection of small molecule and protein combing with aptamer.

View Article Online
DOI: 10.1039/C8AN00437D

2. EXPERIMENTS

2.1 Reagents

DNA oligonucleotides were designed and synthesized by Sangon Inc., (Shanghai, China) and TaKaRa Bio Inc. (Dalian, China). The detailed sequences are listed in Table 1. Bovine serum albumin (BSA), streptavidin–alkaline phosphatase (ST-ALP), a-naphthyl phosphate (a-NP), 6- Mercapto-1-hexanol (MCH) and salmon sperm DNA were purchased from Sigma-Aldrich (USA). dNTP and agarose were purchased from Takara (Dalian, China). All other reagents were of analytical reagent grade. And all the consumable items were treated by 1% DEPC and sterilized three times. Piranha solution contained 98% concentrated sulfuric acid and 30% hydrogen peroxide (75/25, *v/v*). TNaK buffer is the hybridization buffer (pH7.5) contained 20 mM Tris, 140 mM NaCl, 5.0 mM KCl. Tris-HCl buffer is washing buffer (pH7.4) contained 20 mM Tris, 0.10 M NaCl, 5.0 mM $MgCl_2$ and 0.05% Tween-20. Diethanolamine (DEA) buffer (pH9.6) contained 0.1 M DEA, 1 M $MgCl_2$ and 100 mM KCl. The Millipore-Q water ($\geqq$18 MΩ cm^{-1}) was used in all experiments.

2.2 Apparatus

All electrochemical experiments were performed by the CHI660D electrochemical workstation (Shanghai Chenhua Instruments Co., Ltd., China) with a conventional three electrode system composed of platinum wire as auxiliary, Ag/AgCl electrode as reference, platinum electrode as counter electrode and a 3 mm diameter gold electrode as working electrode. Desktop low-temperature high-speed centrifuge (Heraeus, Germany), HH-W420 electric-heated thermostatic water bath (Hengfeng, China), and KQ3200DB ultrasound equipment (Kunshan, China) were also used for the experiment.

View Article Online
DOI: 10.1039/C8AN00437D

2.3 Preparation of electrochemical biosensor

The bare gold electrode was chasing by 50 nm alumina slurries and treated in ultrapure water by ultrasound for a few minutes, followed by infiltration in piranha solution for 10 min to eliminate other substances. The preprocessed gold electrode was rinsed with ultrapure water and allowed to dry at room temperature. 10 μL of thiolated capture probe at 0.2 μM was dropped onto the pretreated gold electrode surface and hatched over night at 4 ^{o}C. After washed with the Tris-HCl buffer, the electrode was blocked into 100 μL of 1 mM MCH for 1 h and 37^{o}C to achieve well-aligned DNA monolayer which can occupy the left bare sites. The electrode was further rinsed with the washing buffer and treated in salmon sperm DNA and 1% BSA for 30 min to block the non-specific binding sites on its surface to avoid the nonspecific adsorption of the other DNA or enzyme.

CHA system included miR-21, biotin labeled hairpin probes (H1 and H2), TNaK buffer, RNAase inhibitor, and DEPC-treated water. The final concentration of RNAase inhibitor was 1 U μL^{-1}. After 0.5 h amplification reaction, the products hybridized with the capture probes were immobilized on the gold electrode for 0.5 h at 37 °C. Then 10 μL of 1 nM streptavidin (SA) dissolved in PB buffer was added on the gold electrode and reacted for 0.5 h at 37 °C, armed to combine with the biotin at the end of CHA product. Finally, the gold electrode was washed by washing solution.

Then the RCA was carried out. In RCA experiment, 10 mM cyclic DNA template and 10 nM DNA primer labeled with biotin were dissolved in PB buffer to make the mixed system. Then 10 μL of this mixed system was added to biosensor and reacted for 0.5 h at 37°C. Therefore, the cyclic DNA template and DNA primer were combined to CHA product by biotin and streptomycin affinity reaction. After the biosensor was thoroughly washed with washing buffer, 10 μL RCA reaction buffer

View Article Online
DOI: 10.1039/C8AN00437D

(33 mM, pH 7.9 Tris-HCl buffer) coupled with 0.4 U phi29 DNA polymerase were dropped onto biosensor surface and incubated for 1 h at 37 °C. After the amplification, 10 μL 1 μM biotin labeled probe was dropped onto the biosensor to react for 1 h at 37 °C, which made the probe combining with the RCA product.

Following washed by DEA buffer containing 0.05% Tween-20, 10 μL of 0.5 μg mL^{-1} streptavidin labeled ST-AP was dropped onto the electrochemical biosensor at 37 °C for 0.5 h, and wasted thoroughly with DEA buffer containing 0.05% Tween-20. The differential pulse voltammetry (DPV) measurement was performed in DEA buffer containing 1 mg mL^{-1} of α-NP substrate with initial potential 0 V; terminal potential 0.6 V; potential increment 0.005 V; amplitude 0.07 V; pulse width 0.06 s; sample width 0.016 s; standing time 2 s.

3. RESULTS AND DISCUSSION

3.1 Design of the electrochemical biosensor

The strategy of the fabricated electrochemical biosensor platform for the detection of miRNA 21 has been shown in figure 1. In this method, miRNA 21 has been amplified and detected through dual-amplification, involving CHA and RCA. MiRNA 21 firstly experienced the CHA amplification. Before amplification, H1 was labeled by biotin. Then biotin labeled H1H2 hybrid duplex was formed in the presence of objective miRNA 21. In addition, this biotin labeled hybrid duplex was captured by probes on the gold electrode. The primer of RCA was also labeled by biotin and subsequently combined with the CHA product by streptavidin. Later on, dNTP and Phi29 DNA polymerase were added to start the rolling circle amplification. After amplification, the generated linear repeating sequences which complement to the template were associated with the biotin labeled detection probes. Finally, these

View Article Online
DOI: 10.1039/C8AN00437D

RCA products were linked to the streptavidin labeled ST-AP to catalyze the α-NP and produce the electrochemical signals.

3.2 Characterization of electrode surface modification

Electrochemical impedance spectroscopy (EIS) and square wave voltammetry (SWV) measurements were adopted to evaluate the modification of electrochemical biosensor in each step. The EIS curves were achieved in 0.4 M KCl containing 0.5 mM $Fe(CN)_6^{3-/4-}$ and the diameter of semicircle was equal to electron-transfer resistance (Ret) (Fig. 2A). In 0.4 M KCl containing 0.5 mM $Fe(CN)_6^{3-/4-}$, bare electrode exhibited an almost straight line (curve a) because of electron free transfer, which was reflecting the outstanding electrochemical conductivity. When the thiolated capture DNA was self-assembled onto the bare electrode through Au-thiol binding, the electron transfer was limited and the Ret increased (curve b). This was because that the negatively charged phosphate backbone of the oligonucleotides produced an electrostatic repulsion force to $[Fe(CN)_6]^{3-}/[Fe(CN)_6]^{4-}$. However, after MCH and BSA were immobilized onto the electrode surface, the Ret increased obviously (curve c), on account of that the bio-macromolecules could obstruct the electron transfer. Afterwards the remaining capture DNA hybridized with the H1-H2 complexes without the participation of target miRNA, the Ret slightly increased (curve d). With participation of target miRNA, the Ret increased significantly (curve e), which indicated that only a few of H1 and H2 can initiate reaction in the absence of the target, and in the presence of target miRNA catalysis, a large amount of H1–H2 complexes were obtained. These results were in a good agreement with those obtained from SWV measurements (Fig. 2B), in which the peak currents varied upon the

View Article Online
DOI: 10.1039/C8AN00437D

assembly and binding processes. Both results of EIS and SWV proved that the biosensor worked indeed as described in the principle scheme.

3.3 Optimization of experiment conditions

We have investigated different experiment to achieve the optimal sensing performance, containing the incubating time of CHA (Figure 3A), the incubating time of RCA (Figure 3B), the proportion of H1 and H2 (Figure 3C) and the concentration of streptavidin. The signal-to-noise ratio has been used for the evaluation of the electrochemical biosensor performance. From the figure 3A, the signal-to-noise ratio went up with the increment of incubating time and reached the maximum at 30 min, demonstrating that the optimized reaction time of target miRNA from CHA amplification was 30 min. In addition, the proportion of H1 and H2 is another significant factor for the CHA amplification. As shown in figure 3B, the optimized proportion of H1 and H2 was 1:1 (molar ratio), when the signal-to-noise ratio was 20. Besides CHA, the conditions of RCA has also been optimized. As shown in figure 3B, the signal-to-noise ratio outstandingly increased before 60 min, and reached a peak at 60 min. Therefore, the optimum incubating time of RCA was 60 min. Finally, the concentration of streptavidin was investigated and the signal-to-noise ratio reached to the maximum when the concentration was 1 nM.

3.4 Analytical performance of miRNA detection

Under the optimum conditions of experiment, the capability of prepared electrochemical biosensor was explored by the measurement of DPV peak currents, such as the dynamic range and sensitivity. From the figure 4A, the DPV peak currently increased (from a to f) following the augment of the target miRNA 21

View Article Online
DOI: 10.1039/C8AN00437D

concentration. Additionally, it showed the excellent linearity between the peak currents and the logarithm of target miRNA 21 concentrations from the range of 0.5 pM to 12.5 nM. The limit of detection is 290 fM. The resulting linear equation was ip (μA) = 1.89+3.14log C_{miRNA} (the unit is pM) with the correlation coefficient of 0.9953. Compared to the traditional method involving Northern blot, PT-PCR, and the other reported electrochemical biosensors, the results above showed the wider linear range and higher sensitivity. (Shown in Table S1) Moreover, two concentrations, 1.25 pM and 1.25 nM, have been used for the investigation of the repeatability. And the result showed that both of them had good reproducibility with the coefficient of variation less than 5%.

3.5 Specificity of the proposed sensor

We evaluated the specificity of the proposed electrochemical biosensor by detecting four different kinds of control oligonucleotides and a blank control, containing complete sequence complementary of target miRNA 21, single-base mismatched oligonucleotide, double-base mismatched oligonucleotide, and non-complementary oligonucleotide. The DPV currents and DPV signal curve of these oligonucleotides were measured with the concentration of 125 pM under the optimized detection conditions. As the result (figure 5), the signal responses of single-base mismatched oligonucleotide, double-base mismatched oligonucleotide, and non-complementary oligonucleotide were all as similar as that of the blank control, which were less than 20% of full complementary sequence of target miRNA 21. Therefore, this electrochemical biosensor was probable for the effective detection of the target miRNA 21 with high specificity and had potential for the practical analysis.

View Article Online
DOI: 10.1039/C8AN00437D

3.6 Real sample analysis

After the characterization, our designed electrochemical biosensor was investigated in real sample analysis to demonstrate its capability. This miRNA assay was performed by using human Hela cell RNA. The RNA was extracted by trizol method after the cell counting. And the sensitivity of our method was explored by cell concentration from 10^2 to 10^7 cells. As the result, the sensitivity in the analysis of Hela cell RNA was reached to low concentration at 10^3 cells. The linearity was excellent with the R values greater than 0.99, which corresponded to the calibration curve of the standard miRNA 21. (Figure 6) This result indicated that our designed electrochemical biosensor can serve as the promising tool for the detection of miRNA 21 in real bio-samples with great sensitivity, accuracy, and reliability.

4. CONCLUSIONS

In this work, we have designed a novel highly sensitive and specific detection of microRNA 21 method, based on catalytic hairpin assembly coupled with rolling circle amplification. In this strategy, the CHA was combined with RCA by biotin-streptavidin affinity reaction, which improved the sensitivity of the miRNA detection with the 290 fmol LOD and an excellent performance in real sample analysis with a good linear of 0.5~12500 pmol. This method also indicated preferable specificity. Although there has had several relative works for detection of miRNA, our strategy can achieve high sensitivity conveniently just by combining the CHA and RCA method.[33-35] Therefore, this proposed electrochemical biosensor can detect the miRNA in biomedical research and even early clinical diagnosis.

View Article Online
DOI: 10.1039/C8AN00437D

ACKNOWLEDGEMENTS

We appreciate the support of National Natural Science Foundation of China, No.21505116. The work was also supported by the scientific research funds of talents from Xuzhou Medical University, No. D2015014.

CONFILICT OF INTEREST

The authors declare that they have no conflict of interest.

REFERENCES

[1] K. Chaudhuri, R. Chatterjee, DNA Cell Biol., 2007, **26**, 321-337.

[2] C. Hilton, F. Karpe, Clin. Chem., 2013, **59**, 729-731.

[3] H. Guo, N. T. Ingolia, J. S. Weissman, D. P. Bartel, Nature, 2010, **466**, 835-40.

[4] D. Baek, J. Villén, C. Shin, F. D. Camargo, S. P. Gygi, D. P. Bartel, Nature, 2008, **455**, 64-71.

[5] T. S. Elton, H. Selemon, S. M. Elton, N. L. Parinandi, Gene, 2013, **532**, 1-12.

[6] K. A. Cissell, S. Shrestha, S. K. Deo, Anal.Chem., 2007, **79**, 4754-4761.

[7] M. Planell-Saguer, M. C. Rodicio, Z. Mourelatos, Nat Protocl., 2010, **5**, 1061-1073.

[8] J. Koshiol, E. Wang, Y. Zhao, F. Marincola, M. T. Landi, Cancer Epidemiol Biomarkers Prev., 2010, **19**, 907-911.

[9] I. Lee, S. S. Ajay, H. Chen, A. Maruyama, N. Wang, M. G. McInnis, B. D. Athey, Nucleic Acids Res., 2008, **36**, e27.

[10] Z. Qiu, J. Shu, D. Tang, Anal. Chem., 2018, **90**, 1021-1028.

View Article Online
DOI: 10.1039/C8AN00437D

[11] J. Shu, Z. Qiu, S. lv, K. zhang, D. Tang, Anal. Chem., 2018, **90**, 2425-2429.

[12] K. Zhang, S. Lv, Z. Lin, M. Li, D. Tang, Biosens. Bioelectrorn., 2018, **101**, 159-166.

[13] Q. Zhou, Y. Lin, K. Zhang, M. Li, D. Tang, Biosens. Bioelectron., 2018, **101**, 146-152.

[14] P. Mestdagh, T. Feys, N. Bernard, S. Guenther, C. Chen, F. Speleman, J. Vandesompele, Nucleic Acids Res., 2008, **36**, e143.

[15] L. Yan, J. Zhou, Y. Zheng, A. S. Gamson, B. T. Roembke, S. Nakayama, H. O. Sintim, Mol Biosyst., 2014, **10**, 970-1003.

[16] R. A. McDonald, K. M. White, J. Wu, B. C. Cooley, K. E. Robertson, C. A. Halliday, J. D. McClure, S. Francis, R. Lu, S. Kennedy, S. J. George, S. Wan, van Rooij E, A. H. Baker, Eur Heart J., 2013, **22**, 1636-1643.

[17] J. A. Chan, A. M. Krichevsky, K. S. Kosik, Cancer Res., 2005, **65**, 6029-6033.

[18] F. Meng, R. Henson, H. Wehbe-Janek, K. Ghoshal, S. T. Jacob, T. Patel, Gastroenterology, 2007, **133**, 647-658.

[19] F. Y. Zhou, Y. Yao, J. J. Luo, X. Zhang, Y. Zhang, D. Y. Yin, F. L. Gao, P. Wang, Analytica Chimica Acta, 2017, **969**, 8-17.

[20] F. L. Gao, Y. Qian, L. Zhang, S. Z. Dai, Y. F. Lan, Y. Zhang, L. Du, D. Q. Tang, Biosens. Bioelectron., 2015, **71**, 158-163.

[21] Y. Qian, C. Wang, F. L. Gao, Biosens. Bioelectron., 2015, **63**, 425-431.

[22] Y. Yu, C. Yu, T. Yin, S. Ou, X. Sun, X. Wen, L. Zhang, D. Q. Tang, X. X. Yin, Biosens. Bioelectron., 2017, **87**, 278-284.

[23] D. X. Nie, Z. Han, Y. Y. Yu, G. Y. Shi, Sensors and Actuators B-Chemical, 2016, **224**, 584-591.

[24] T. Hou, W. Li, X. Liu, F. Li, Anal. Chem., 2015, **22**, 11368-11374.

View Article Online
DOI: 10.1039/C8AN00437D

[25] X. Liu, W. Li, T. Hou, S. Dong, G. Yu, F. Li, Anal. Chem., 2015, **87**, 4030-4036.

[26] Y. Tan, X. Wei, Y. Zhang, P. Wang, B. Qiu, L. Guo, Z. Lin, H. Yang, Anal. Chem., 2015, **23**, 11826-11831.

[27] W. Li, X. Liu, T. Hou, H. Li, F. Li, Biosens. Bioelectron., 2015, **71**, 304-309.

[28] F. Xuan, X. Luo, I. Hsing, Biosens. Bioelectron., 2012, **1**, 230-234.

[29] G. Wang, X. He, L. Chen, Y. Zhu, X. Zhang, L. Wang, Biosens. Bioelectron., 2013, **50,** 210-216.

[30] G. Xiang, D. Jiang, F. Luo, F. Liu, L. Liu, X. Pu, Sens. Actuators Chemical-B, 2014, **195**, 515-519.

[31] K. Ren, J. Wu, F. Yan, H. Ju, Sci. Rep., 2014, **4**, 4360-4365.

[32] Y. He, X. Wang, J. Sun, S. Jiao, H. Chen, F. Gao, L. Wang, Anal. Chim. Acta, 2014, **810**, 71– 78.

[33] R. Deng, K. Zhang, J. H. Li, Acc. Chem. Res., 2017, **50**, 1059-1068.

[34] Q. Tian, Y. Wang, R. Deng, L. Lin, Y. Liu, J. H. Li, Nanoscale, 2015, **7**, 987-993.

[35] R. Deng, L. Tang, Q. Tian, Y. Wang, L. Lin. J. H. Li, Angew. Chem. Inter. Ed., 2014, **53**, 2389-2393.

View Article Online
DOI: 10.1039/C8AN00437D

Figure captions

Figure 1. Principle of the electrochemical biosensor for detection of miRNA

Figure 2. EIS（A）and SWVs（B）at different electrodes in 0.4 M KCl containing 0.5mM[Fe(CN)6]4-/3 at bare electrode (a), capture DNA modified electrode (b), MCH and BSA immobilized on the electrode surface (c), after hybridized with H1-H2 complexes with target miRNA(d) ,after RCA (e).

Figure 3. (A) Dependenec of DPV peak currents on reaction time of CHA; (B) reaction time of RCA; (C) ratio of H1 to H2; and (D) streptavidin concentration.

Figure 4. (A) DPV response to 0.5, 1.25, 12.5, 125, 1250, 12500pM target miRNA(from a to h). (B) Plot of DPV peak current vs. logarithm of target miRNA concentration. The error bars represent the standard deviations in three different measurements for each concentration.

Figure 5. DPV peak currents (A) and typical DPV curvesand (B) respectively respond to 125pM of target miRNA(a), Single-base-mismatched oligonucleotide (b), Two-base-mismatched oligonucleotide (c), Non-complementary oligonucleotide (d), and blank(e).

Figure 6. Application of the biosensor in Hela cell line and data analysis, curve a stands for the concentration of miRNA and curve b stands for the count of Hela cell.

View Article Online
DOI: 10.1039/C8AN00437D

Table 1. Sequences of the used oligonucleotides (in 5′ to 3′ direction)

Oligonucleotide	**Sequence (5′- 3′)**
Capture probe	SH-$(CH_2)_6$-TTTTGAGTAGAGTCTGA
MicroRNA-21	UAGCUUAUCAGACUGAUGUUGA
Hairpin probe 1 (H1)	Biotin-TTTTCAACATCAGTCTGATAAGCTACCATGTGTAGAT
	AGCTTATCAGACTCTACTCA
Hairpin probe 2 (H2)	TAAGCTATCTACACATGGTAGCTTATCAGACTCCATGTGTAGA
Primer-RCA	AAAAAAAAACACAGCTGAGGATAGGACAT
Circle template	P-CTCAGCTGTGTAACAACATGAAGATTGTAGGTCAGAACTC
	ACCTGTTAGAAACTGTGAAGATCGCTTATTATGTCCTATC
Detection probe	TCAGAACTCACCTGTTAGTTTTTT-Biotin
Single-base-mismatched oligonucleotide	UAGCUUAUCAUACUGAUGUUGA
Two-base-mismatched oligonucleotide	UAGCUUAUCAUACUGACGUUGA
Non-complementary oligonucleotide	GCUAUCCGUCAGUGUAUAGCGC

View Article Online
DOI: 10.1039/C8AN00437D

Figure 1.

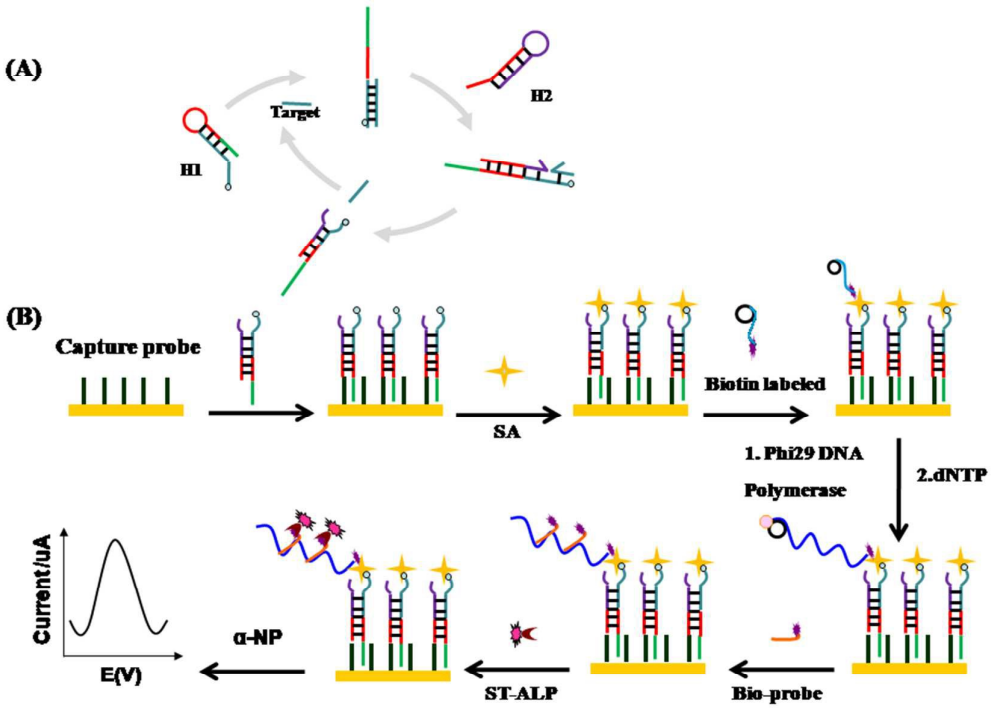

View Article Online
DOI: 10.1039/C8AN00437D

Figure 2.

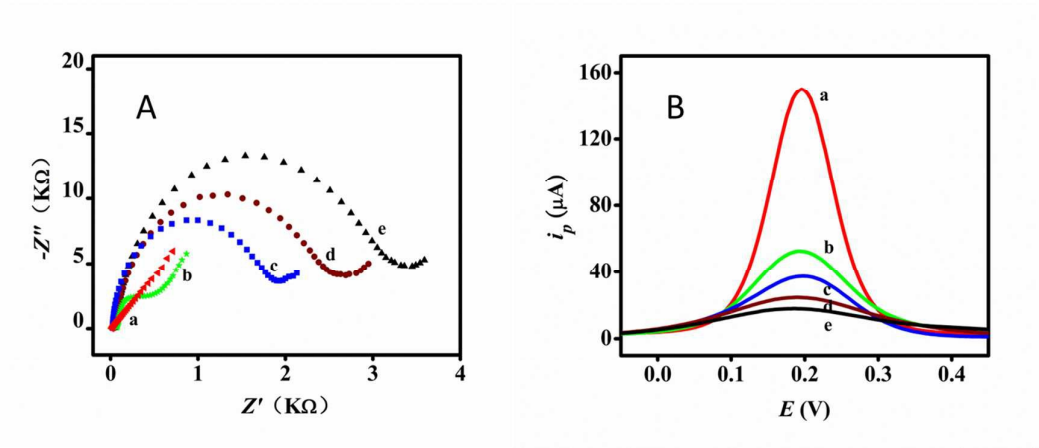

View Article Online
DOI: 10.1039/C8AN00437D

Figure 3.

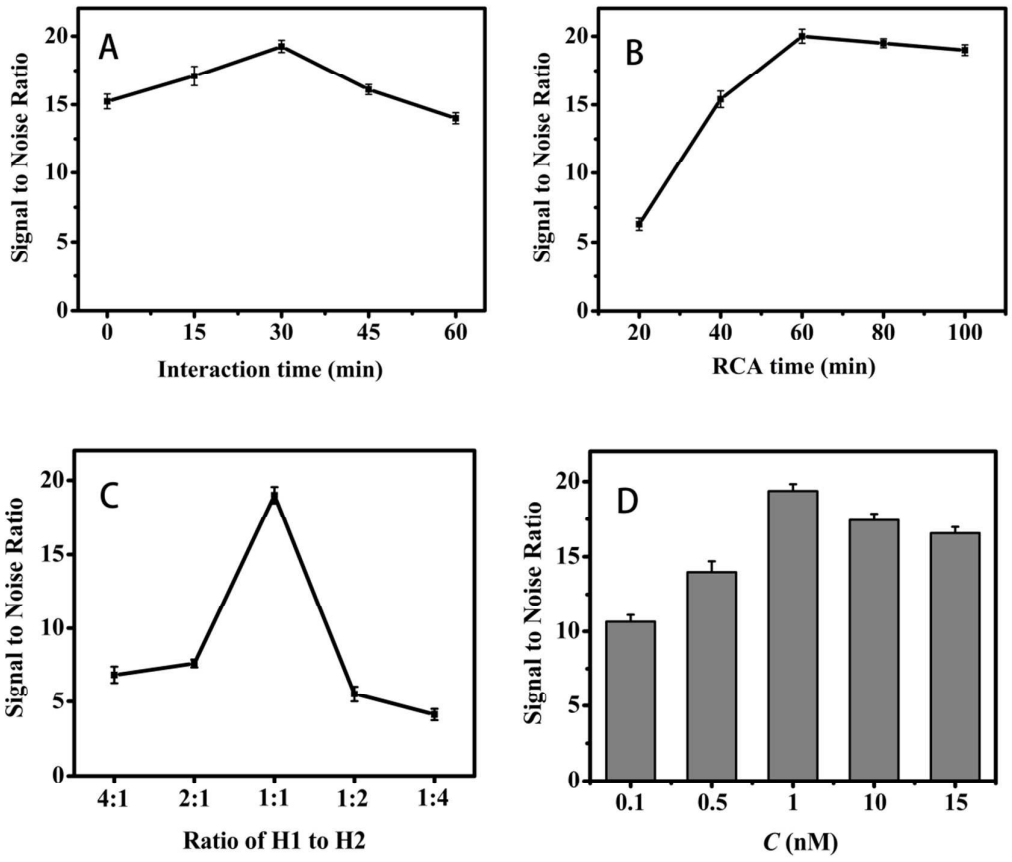

View Article Online
DOI: 10.1039/C8AN00437D

Figure 4.

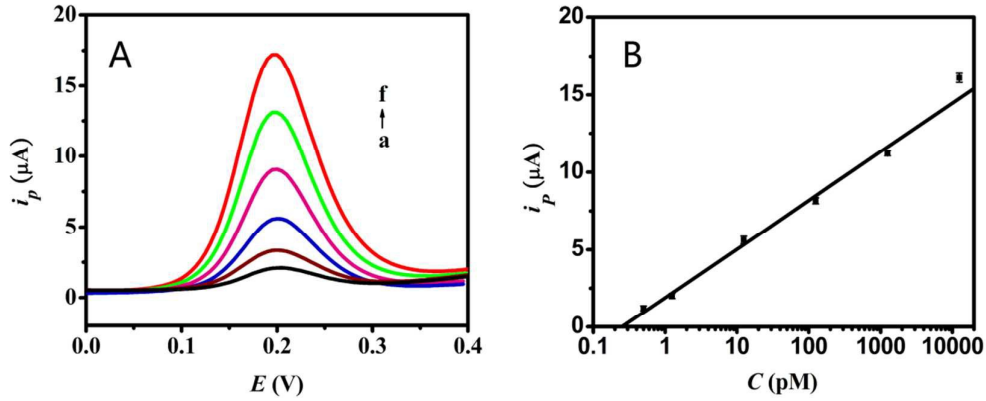

View Article Online
DOI: 10.1039/C8AN00437D

Figure 5.

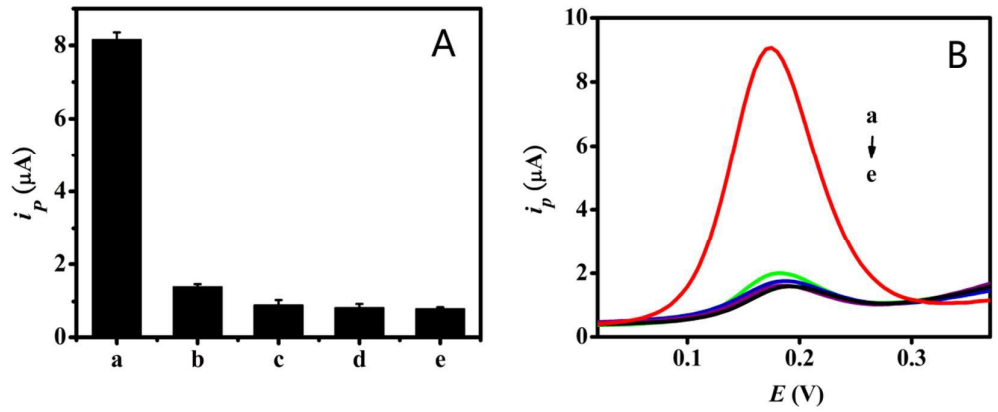

View Article Online
DOI: 10.1039/C8AN00437D

Figure 6.